JOURNAL OF GEOPHYSICAL RESEARCH, VOL. 90, NO. D6, PAGES 10,541–10,550, OCTOBER 20, 1985

Improvements to the Algorithm for Computing CO_2 Transmissivities and Cooling Rates

M. DANIEL SCHWARZKOPF AND STEPHEN B. FELS

Geophysical Fluid Dynamics Laboratory/NOAA, Princeton University, New Jersey

A new interpolation algorithm is derived for obtaining CO_2 15-μm transmissivities at any pressure from tables of transmission functions at standard pressures. The new method is a revision of the Fels-Schwarzkopf (1981) technique. Improvements to the standard transmissivity tables are also discussed. An extension of these methods to calculate transmissivities at CO_2 concentrations other than those used for the tables is described.

1. INTRODUCTION

Fels and Schwarzkopf [1981] (hereinafter referred to as FS) have published a method for the efficient and accurate calculation of CO_2 15-μm band transmissivities and cooling rates. In this approach, transmission functions are precomputed using a detailed line-by-line procedure on a fixed pressure grid for three standard temperature profiles at CO_2 mixing ratios of 330 and 660 ppmv. An interpolation scheme is provided to allow the determination of transmissivities, for each temperature profile, at any two pressures p and p'. A further interpolation obtains the transmissivity at any specified temperature profile. Cooling rates may be computed from these transmissivities after correcting for the variation of the Planck function across the width of the 15-μm band.

Since their publication the tables and algorithms of FS have been used for a number of different purposes: (1) as was originally envisioned, for the calculation of cooling rates in general circulation models; (2) for calculating radiative damping rates for waves of various scales in the stratosphere; and (3) as a reference standard for various more highly parameterized calculations.

All of these applications require the accurate computation of transmissivities at arbitrary pressures by means of an interpolation scheme. Our own experience, and that of other users, has shown that an improvement of this interpolation scheme would be desirable, especially for uses which require transmissivities for small paths. It is also clear that the utility of the method for all purposes would be enhanced if it could be used at arbitrary mixing ratios rather than only at the standard 330- and 660-ppmv cases. Finally, it is obvious that the line-by-line calculations ought to make use of the best available spectroscopic data.

In light of the above considerations, we have completely revised both the precomputed tables of transmission functions and the method of interpolating these to user-defined pressures. In addition, we have developed a procedure for computing transmissivities at concentrations other than those of the tables. It is the purpose of this short paper to describe these improvements.

2. CHANGES TO THE PRECALCULATED TRANSMISSIVITY TABLES

2.1. *Changes in Line Data*

The line-by-line calculations of FS include 19 bands of the CO_2 fundamental and 8 isotopic bands, comprising about 3800 lines (see Table 7 of FS). In this revision we have included all CO_2 lines listed in the 1980 Air Force Geophysics Laboratory compilation [*Rothman*, 1981]. Lines less than 0.01 cm^{-1} apart in frequency are combined, with a weighted line width and a summed line strength being employed. The total number of lines thus becomes about 12,500.

Line-by-line (LBL) computations using the revised data are performed exactly as in the work of FS. We note, in particular, that all lines are cut off at a distance of 3 cm^{-1} from the line center; the effects of this assumption, as well as a comparison with experimental data [*Gryvnak et al.*, 1976; *Gryvnak and Burch*, 1978] have been reported by FS (p. 1226). The actual choice of the cutoff value is not critical; our results, as published in the WMO intercomparison of radiation codes [*World Climate Programme*, 1984] agree closely with those of other investigators, despite the adoption of different formulations of the cutoff. For example, downward fluxes at the surface computed by the various investigators agree to within 2%. In a future paper we will discuss our LBL results in greater detail.

Results of these revised calculations show a fractional increase in absorption of about 1% at pressures of 10–100 mbar and increases of lesser amounts at other pressures. This result is consistent with random model calculations discussed by FS.

2.2. *Changes in the Transmissivity Tables*

For each standard temperature sounding, two tables of transmissivities were employed by FS. The upper table was used to interpolate between any two user-defined pressures whenever both such pressures were less than or equal to 10 mbar; the lower table was used in all other cases. This approach introduces inaccuracies in the computation of transmissivities between two pressures when the larger pressure is greater than 10 mbar and the smaller is less, since the lower transmission function table, on a coarse pressure grid, must be employed. As an indication of the error, the difference in transmissivities between 10 mbar and the top of the atmosphere using the upper and lower tables is 0.000004. Although this number is rather small, one should note that the effect on heating rates near 10 mbar is larger; the fractional error in heating rates will equal this error divided by the change in the transmission function, a considerably larger quantity.

In this revision we have calculated all transmissivities on one pressure grid, thus eliminating the error described above. The smallest nonzero pressure for which transmissivities are calculated is 0.001 mbar. Fifteen pressure levels are included for each tenfold increase of pressure, spaced evenly in the logarithm of pressure. For pressures between 100 and 1000 mbar, 30 pressure levels are included, similarly spaced. Two

Paper number 5D0543.

pressure levels greater than 1000 mbar are included. The temperature profile used in these calculations is the U.S. Standard Atmosphere (1976), as smoothed using the procedure described by S. B. Fels (manuscript in preparation, 1985), with the temperature taken to be the mass-averaged temperature between two standard pressure levels. Above the mesopause an isothermal profile is used. Table 1 is a complete list of the standard temperatures, pressures and geometric heights employed. Unlike those of FS, the temperature profiles for all standard CO_2 concentrations are identical.

The choice of this pressure scale is prompted by several considerations. First, the pressures are spaced an equal fraction of a scale height apart at all altitudes. Above 100 mbar, each level is $\sim$0.15 scale height or $\sim$1 km apart. Disturbances with wavelengths greater than $\sim$6 km will be directly resolved by this grid. This resolution is sufficient for the most important waves in the middle atmosphere. (The interpolation scheme to be described will produce transmissivities for smaller intervals between pressure levels.) By contrast, the pressure grid of FS is unevenly spaced in scale height. Second, the accuracy of interpolation is improved. For large paths, CO_2 absorption is observed to be proportional to the logarithm of absorber amount [*Howard et al.*, 1956]; hence transmissivities between a reference pressure level and other pressure levels spaced logarithmically will vary approximately linearly.

In addition, the lower limit of pressures has been raised to 0.001 mbar, corresponding to a geometric height of $\sim$93 km. The number of levels above the mesopause has been increased from 2 to 15, permitting more accurate calculations in those regions. At the lowest pressures the transmissivities obtained approach those calculated in the weak line limit (see Figure 1).

2.3. *Unweighted Transmissivities*

The transmissivity tables defined by FS contain precomputed "Planck-weighted" transmission functions defined as

$$\tau(p, p'; 250) = \int \tau_\nu(p, p') B_\nu(250)\, d\nu \Big/ \int B_\nu(250)\, d\nu \qquad (1)$$

The integration has been performed (in finite difference form) over the entire 15-μm band (taken to be from 500 to 850 cm^{-1}) using 10-cm^{-1} frequency intervals. $B_\nu(250)$ is the Planck function evaluated at 250 K. For comparison with experimental or other computational procedures it is useful to have available the unweighted transmission function

$$\tau(p, p') = \frac{1}{\Delta\nu} \int \tau_\nu(p, p')\, d\nu \qquad (2)$$

The integral is computed in the same manner as in (1). In this revision we have provided the user with tables of both the Planck-weighted and the unweighted transmissivities. The interpolation method discussed in section 3 applies equally to both types of transmissivities.

2.4. *Cooling Rates*

Planck-weighted transmissivities have been employed to obtain cooling rates for the standard temperature and pressure profile. The CO_2 mixing ratio is taken as 330 ppmv, and the atmosphere is assumed to be in local thermodynamic equilibrium (LTE). The right-hand column of Table 1 gives cooling rates for the 108 levels of the pressure grid. These values differ somewhat from those given by FS (Table 12) at 49.5, 53.0, and 56.5 km, primarily owing to the different standard temperature profile adopted for this revision. Above $\sim$70 km these cooling rates became inaccurate owing to the LTE assumption.

3. THE INTERPOLATION ALGORITHM

3.1. *The General Scheme*

A completely new interpolation algorithm for obtaining $\tau(p, p')$ at user-defined levels has been constructed for use with the revised tables. The new scheme is better than that used by FS in two important respects: (1) it produces more accurate results in the case that $\Delta p \equiv |p - p'|$ is small in comparison with the average pressure $\bar{p}$, and (2) it yields a smoother interpolation and insures that $\tau(p, p')$ decreases with increasing Δp.

In this method we construct an analytic function $A(p, p')$, an approximation to the actual absorptivity $a(p, p') = 1 - \tau(p, p')$. When evaluated on the standard pressure grid, this gives a set of values $A(p_i, p_j)$. We denote by $E(p_i, p_j)$ the difference $a(p_i, p_j) - A(p_i, p_j)$. This difference function should be both small and smooth, since $A(p, p')$ has been constructed to include as nearly as possible the nonlinearities of $a(p, p')$. It is therefore possible to compute $E(p, p')$ from the relevant values of $E(p_i, p_j)$ by means of a quadratic interpolation. The interpolated absorptivity may then be evaluated as

$$a(p, p') \cong E(p, p') + A(p, p') \qquad (3)$$

The most important aspect of this scheme is the specification of $A(p, p')$. In the appendix we obtain the following expression for $A(p, p')$:

$$A(p, p') = \{C(p) \log [1 + X(p)U(p, p')^{0.90}]\}^{\gamma(p)} \qquad (4)$$

where

$$U(p, p') = \frac{\Delta p^{1/\gamma}(p + p' + 5)}{\eta(p + p' + 5) + \Delta p^{(1/\gamma - 1)}} \qquad (5)$$

In (4) and (5), $U(p, p')$ is a path function which, roughly speaking, corresponds to the pressure-weighted absorber amount between p and p'. $C(p)$, $X(p)$, $\gamma(p)$, and $\eta(p)$ are empirical coefficients which are not functions of the path; consequently they may be precomputed for the standard pressures given in Table 1, then evaluated at p by linear interpolation. We also assume $p > p'$ and have defined the numerical constants and coefficients so that all pressures are expressed in mbar. The choices of these constants and of the empirical coefficients in (4) and (5) are designed to correspond to various experimental constraints, as is discussed in the appendix.

Two important observations should be made at this point. First, we emphasize that the user wishing to apply our method need not be concerned with the detailed derivations of (4) and (5) given in the appendix. Second, the approximation formulas are derived to be most accurate in the special circumstances of small Δp with widely varying $\bar{p}$ and should not be used generally as a method for estimation of transmissivities. In fact, fractional errors of up to 30% have been obtained by the direct application of (4) and (5) to compute absorptivities on the 41-level pressure grid discussed in section 5.

3.2. *Application to Closely Spaced Pressures*

In certain situations the user may desire transmissivities between two pressures more closely spaced than the standard pressure grid. More precisely, if we let p, p' be the user-specified pressures and $p(i)$, $p(j)$ be the corresponding standard pressures for which

$$p(i) \le p \qquad p(i + 1) > p$$

$$p(j) \le p' \qquad p(j + 1) > p'$$

TABLE 1. Standard Pressures (in Millibars) and Temperatures Used to Compute the CO_2 Transmissivity Tables

Index i	Pressure, mbar	Temperature, K	Height, km	Cooling Rate, deg d^{-1}
1	0	186.9	∞	−28.47
2	0.00100	186.9	93.4	−12.36
3	0.00117	186.9	92.6	−10.39
4	0.00136	186.9	91.7	−8.57
5	0.00158	186.9	90.8	−6.90
6	0.00185	186.9	90.0	−5.35
7	0.00215	187.0	89.1	−3.91
8	0.00251	187.0	88.2	−2.53
9	0.00293	187.1	87.4	−1.32
10	0.00341	187.6	86.5	−0.57
11	0.00398	188.7	85.6	−0.59
12	0.00464	190.3	84.8	−0.98
13	0.00541	192.0	83.9	−1.32
14	0.00631	193.7	83.0	−1.54
15	0.00736	195.4	82.1	−1.66
16	0.00858	197.2	81.2	−1.74
17	0.0100	199.0	80.3	−1.79
18	0.0117	200.8	79.4	−1.84
19	0.0136	202.6	78.5	−1.87
20	0.0158	204.4	77.5	−1.91
21	0.0185	206.3	76.6	−1.94
22	0.0215	208.1	75.6	−1.96
23	0.0251	210.0	74.7	−1.96
24	0.0293	211.9	73.7	−1.94
25	0.0341	213.9	72.7	−1.94
26	0.0398	216.3	71.8	−2.08
27	0.0464	218.9	70.8	−2.34
28	0.0541	221.7	69.8	−2.60
29	0.0631	224.5	68.7	−2.84
30	0.0736	227.3	67.7	−3.06
31	0.0858	230.2	66.7	−3.27
32	0.100	233.1	65.6	−3.48
33	0.117	236.1	64.5	−3.68
34	0.136	239.1	63.5	−3.90
35	0.158	242.1	62.4	−4.12
36	0.185	245.2	61.3	−4.37
37	0.215	248.3	60.1	−4.65
38	0.251	251.4	59.0	−4.97
39	0.293	254.6	57.8	−5.35
40	0.341	257.8	56.7	−5.79
41	0.398	261.1	55.5	−6.31
42	0.464	264.4	54.3	−6.96
43	0.541	267.6	53.1	−7.72
44	0.631	269.9	51.9	−8.24
45	0.736	270.6	50.6	−8.09
46	0.858	270.6	49.4	−7.90
47	1.000	269.9	48.2	−7.69
48	1.17	267.6	46.9	−6.93
49	1.36	264.4	45.7	−6.04
50	1.58	261.2	44.5	−5.30
51	1.85	257.9	43.3	−4.70
52	2.15	254.7	42.2	−4.19
53	2.51	251.5	41.0	−3.75
54	2.93	248.3	39.9	−3.37
55	3.41	245.2	38.7	−3.03
56	3.98	242.2	37.6	−2.72
57	4.64	239.1	36.5	−2.44
58	5.41	236.2	35.4	−2.17
59	6.31	233.2	34.3	−1.91
60	7.36	230.5	33.3	−1.67
61	8.58	228.5	32.2	−1.53
62	10.00	227.2	31.2	−1.48
63	11.7	226.2	30.2	−1.44
64	13.6	225.1	29.1	−1.38
65	15.8	224.1	28.1	−1.30
66	18.5	223.1	27.1	−1.22
67	21.5	222.1	26.1	−1.12
68	25.1	221.1	25.1	−1.03
69	29.3	220.1	24.1	−0.93
70	34.1	219.2	23.1	−0.82
71	39.8	218.2	22.1	−0.71
72	46.4	217.3	21.1	−0.60
73	54.1	216.8	20.1	−0.52
74	63.1	216.7	19.2	−0.46
75	73.6	216.7	18.2	−0.41
76	85.8	216.7	17.2	−0.34
77	100.0	216.7	16.2	−0.30
78	108.0	216.7	15.7	−0.27
79	116.6	216.7	15.2	−0.24
80	125.9	216.7	14.8	−0.21
81	135.9	216.7	14.3	−0.18
82	146.8	216.7	13.8	−0.15
83	158.5	216.7	13.3	−0.12
84	171.1	216.7	12.8	−0.08
85	184.8	216.7	12.3	−0.04
86	199.5	216.7	11.8	0.02
87	215.4	217.1	11.3	0.10
88	232.6	219.5	10.8	0.05
89	251.2	222.6	10.3	−0.02
90	271.2	225.9	9.8	−0.06
91	292.9	229.2	9.3	−0.19
92	316.2	232.6	8.8	−0.11
93	341.5	236.0	8.3	−0.12
94	368.7	239.6	7.8	−0.13
95	398.1	243.0	7.2	−0.14
96	429.9	246.6	6.7	−0.15
97	464.2	250.2	6.1	−0.16
98	501.2	253.9	5.6	−0.16
99	541.2	257.6	5.0	−0.17
100	584.3	261.4	4.4	−0.18
101	631.0	265.3	3.8	−0.18
102	681.3	269.2	3.2	−0.18
103	735.6	273.1	2.6	−0.19
104	794.3	277.2	2.0	−0.19
105	857.7	281.2	1.4	−0.20
106	926.1	285.4	0.7	−0.21
107	1000.0	289.6	0.1	−0.23
108	1079.8	293.8	−0.5	−0.33
109	1165.9	295.9	−1.2	

The geometric height of the pressure levels is given in kilometers. Cooling rates for this sounding with a CO_2 concentration of 330 ppmv are given in the right-hand column.

we now have $p(i) = p(j)$. The relevant values of E, $E[p(i), p(i)]$ and $E[p(i+1), p(i+1)]$ both equal zero; thus $E(p, p') = 0$. According to (3), $a(p, p') = A(p, p')$ in this case.

The absorptivity calculation for these closely spaced layers is thus performed entirely by the use of the approximation function of (4) and (5). Therefore the approximation function needs to be highly accurate for these small values of absorber amount. In the appendix we show that the approximation function is accurate to within 8% for a large range of mean pressures.

4. Changes to Computation of Cooling Rates

4.1. *Layer Transmissivities*

The interpolated transmissivities derived in section 3, as well as those of FS, are "point" transmissivities, i.e., the transmissivity between two specific pressures for a given inhomogeneous path. These transmissivities are most useful for comparison with experimental data or with transmissivities derived by other techniques, such as random models. On the other hand, the quantity required for computation of heating rates at pressure p is

$$\int_{p'=0}^{p_0} \frac{\partial B(p')}{\partial p'} \tau(p', p)\, dp'$$

TABLE 2. Exact and Computed (in Parentheses) Values for the Absorptivity $a(0, p; T)$ for Various Values of Pressure and Temperature

Pressure, mbar	Temperature, K						
	175	200	225	250	275	300	325
0.001	0.000166	0.000171	0.000173	0.000174	0.000175	0.000175	0.000175
	(0.000168)	(0.000172)	(0.000173)	(0.000174)	(0.000174)	(0.000174)	(0.000174)
0.01	0.000463	0.000474	0.000479	0.000481	0.000482	0.000482	0.000481
	(0.000464)	(0.000474)	(0.000479)	(0.000481)	(0.000481)	(0.000481)	(0.000481)
0.1	0.001589	0.001623	0.001640	0.001648	0.001650	0.001649	0.001646
	(0.001589)	(0.001624)	(0.001640)	(0.001648)	(0.001648)	(0.001648)	(0.001648)
1	0.007688	0.007854	0.007937	0.007975	0.007986	0.007983	0.007972
	(0.007689)	(0.007858)	(0.007936)	(0.007975)	(0.007975)	(0.007975)	(0.007975)
10	0.042523	0.043425	0.043874	0.044070	0.044124	0.044098	0.044029
	(0.042493)	(0.043427)	(0.043860)	(0.044073)	(0.044073)	(0.044073)	(0.044073)
100	0.205366	0.209503	0.211530	0.212381	0.212576	0.212406	0.212039
	(0.204780)	(0.209280)	(0.211367)	(0.212392)	(0.212392)	(0.212392)	(0.212392)
315	0.318477	0.324613	0.327661	0.328983	0.329337	0.329150	0.328668
	(0.317209)	(0.324179)	(0.327411)	(0.329000)	(0.329000)	(0.329000)	(0.329000)
1000	0.486218	0.494840	0.499374	0.501588	0.502473	0.502593	0.502279
	(0.483637)	(0.494264)	(0.499192)	(0.501615)	(0.501615)	(0.501615)	(0.501615)

$B_0 = -0.525 \times 10^{-4}$, $B_1 = -0.178 \times 10^{-3}$, $B_2 = -0.110 \times 10^{-5}$, and $B_3 = -0.679 \times 10^{-7}$.

where B is the Planck function. In finite difference form this requires the evaluation of $\tau_{\text{layer}}(p', p)$, where this quantity represents the transmissivity between pressure p and a layer whose average pressure is p'. If the pressure layer around p' is at a very different pressure than p, this layer transmissivity $\tau_{\text{layer}}(p', p)$ differs little from the point transmissivity $\tau(p', p)$. On the other hand, if $p' = p$, the point transmissivity is unity and the layer mean transmissivity is always significantly smaller than 1.

The quantity to be computed may be written as

$$\tau_{\text{layer}}(p', p) = \frac{1}{\Delta} \int_{p'-\Delta/2}^{p'+\Delta/2} \tau(p'', p)\, dp'' \tag{6}$$

where Δ is the difference between the pressures at the top and bottom of the pressure layer. In the new scheme these layer transmissivities may be obtained directly.

The computer program provided to the user allows him to select the option of computing either point transmissivities or layer transmissivities. The layer transmissivities are obtained by a four-point quadrature using Simpson's rule, each evaluation of $\tau(p'', p)$ having been done by means of the interpolation scheme of section 3. For a nearby layer case, where more care is required, a 50-point trapezoidal rule integration is performed.

4.2. *Correction for the Width of the 15-μm Band*

A two-step method has been proposed by FS (section 2*e*) to incorporate the effect of the broad width of the 15-μm band on computation of transmissivities for heating rates. This method involves (1) a precomputation of Planck-weighted transmissivities using equation (1) and (2) correction of these transmissivities for the actual temperature at pressure p by means of a correction function $F(T)$ which is assumed to be pressure independent.

In this revision we have retained this basic method. However, to determine the correction function, we have reevaluated $\tau(p, p'; T)$ for a wider range of temperatures and pressures than was done by FS. We have found that (1) the use of a pressure-independent correction function is justifiable for pressures ranging from 10^{-3} to 10^{3} mbar and (2) the correction function used by FS gives erroneous transmissivities for temperatures below 200 K. Consequently, a new formulation for the correction function has been derived:

$$\tau(p, p'; T) = \tau(p, p'; 250) + F(T)[1 - \tau(p, p'; 250)] \tag{7a}$$

$$F(T) = B_0 + B_1(T - 250) + B_2(T - 250)^2 + B_3(T - 250)^3 \qquad T < 250 \tag{7b}$$

$$F(T) = B_0 \qquad T \geq 250 \tag{7c}$$

The coefficients B_0, B_1, B_2, and B_3 are obtained by means of a least squares fit; B_0, which should equal zero, is negligibly small. Table 2 shows these coefficients as well as predicted and actual transmissivities for $\tau(0, p; T)$ for various values of p and T.

5. Application to Nonstandard CO_2 Mixing Ratios

The interpolation algorithm described in the previous sections requires the use of a table of CO_2 transmissivities at a standard CO_2 mixing ratio. As a result, interpolated transmissivities using our methods may only be obtained at these fixed CO_2 concentrations.

To remedy this shortcoming, we have devised a method enabling the computation of the transmissivity $\tau(p, p'; r)$ between any two specified pressures at CO_2 mixing ratio r by using the transmission function tables at the neighboring standard mixing ratios r_s and r_s'. If the specified pressures are included in the standard pressure grid of Table 1, the interpolation algorithms of sections 3 and 4 may then be applied as before to compute transmissivities at user-defined pressures.

We first observe that for a given temperature path, the transmissivity $\tau(p_1, p_2; r_s)$ depends primarily on the average pressure $\bar{p}$ and on the CO_2 absorber amount $r\Delta p/g$ between p_1 and p_2. Consequently, the transmissivity at a different concentration $\tau(p, p'; r)$ will approximately equal $\tau(p_1, p_2; r_s)$, provided that $\bar{p}$ and $(r\Delta p/g)$ remain unchanged. These constraints lead to the following relations:

$$p_1 + p_2 = p + p' \tag{8a}$$

$$(r_s/r)(p_1 - p_2) = p - p' \tag{8b}$$

(In the above relations we assume that $p > p'$ and $r_s > r$. The latter inequality insures that p_1 and p_2 are never outside the range of the largest and smallest values of p and p'.)

TABLE 3. Fractional Difference in Absorptivity, in Parts Per Thousand, Between Directly Computed Line-by-Line Absorptivity and Interpolated Absorptivity for the 41-Level Pressure Grid Discussed in Section 6

	1	2	3	4	5	6	7	8	9	10	11	12	13	14	15	16	17	18	19	20	21	22	23	24	25	26	27	28	29	30	31	32	33	34	35	36	37	38	39	40	41
1	0	2	1	1	0	0	0	0	0	0	0	0	0	0	0	0	0	0	0	0	0	0	0	0	0	0	0	0	0	0	0	0	0	0	0	0	0	0	0	0	0
2	2	0	0	0	0	0	0	0	0	0	0	0	0	0	0	0	0	0	0	0	0	0	0	0	0	0	0	0	0	0	0	0	0	0	0	0	0	0	0	0	0
3	1	0	0	0	0	0	0	0	0	0	0	0	0	0	0	0	0	0	0	0	0	0	0	0	0	0	0	0	0	0	0	0	0	0	0	0	0	0	0	0	0
4	1	0	0	0	0	0	0	0	0	0	0	0	0	0	0	0	0	0	0	0	0	0	0	0	0	0	0	0	0	0	0	0	0	0	0	0	0	0	0	0	0
5	0	0	0	0	0	0	0	0	0	0	0	0	0	0	0	0	0	0	0	0	0	0	0	0	0	0	0	0	0	0	0	0	0	0	0	0	0	0	0	0	0
6	0	0	0	0	0	0	0	0	0	0	0	0	0	0	0	0	0	0	0	0	0	0	0	0	0	0	0	0	0	0	0	0	0	0	0	0	0	0	0	0	0
7	0	0	0	0	0	0	0	0	0	0	0	0	0	0	0	0	0	0	0	0	0	0	0	0	0	0	0	0	0	0	0	0	0	0	0	0	0	0	0	0	0
8	0	0	0	0	0	0	0	1	0	0	0	0	0	0	0	0	0	0	0	0	0	0	0	0	0	0	0	0	0	0	0	0	0	0	0	0	0	0	0	0	0
9	0	0	0	0	0	0	0	1	0	0	0	0	0	0	0	0	0	0	0	0	0	0	0	0	0	0	0	0	0	0	0	0	0	0	0	0	0	0	0	0	0
10	0	0	0	0	0	0	0	0	0	0	0	0	0	0	0	0	0	0	0	0	0	0	0	0	0	0	0	0	0	0	0	0	0	0	0	0	0	0	0	0	0
11	0	0	0	0	0	0	0	0	0	0	0	0	0	0	0	0	0	0	0	0	0	0	0	0	0	0	0	0	0	0	0	0	0	0	0	0	0	0	0	0	0
12	0	0	0	0	0	0	0	0	0	0	0	0	0	0	0	0	0	0	0	0	0	0	0	0	0	0	0	0	0	0	0	0	0	0	0	0	0	0	0	0	0
13	0	0	0	0	0	0	0	0	0	0	0	0	0	0	0	0	0	0	0	0	0	0	0	0	0	0	0	0	0	0	0	0	0	0	0	0	0	0	0	0	0
14	0	0	0	0	0	0	0	0	0	0	0	0	0	0	1	0	0	0	0	0	0	0	0	0	0	0	0	0	0	0	0	0	0	0	0	0	0	0	0	0	0
15	0	0	0	0	0	0	0	0	0	0	0	0	0	1	0	2	0	0	0	0	0	0	0	0	0	0	0	0	0	0	0	0	0	0	0	0	0	0	0	0	0
16	0	0	0	0	0	0	0	0	0	0	0	0	0	0	2	0	3	0	0	0	0	0	0	0	0	0	0	0	0	0	0	0	0	0	0	0	0	0	0	0	0
17	0	0	0	0	0	0	0	0	0	0	0	0	0	0	0	3	0	2	0	0	0	0	0	0	0	0	0	0	0	0	0	0	0	0	0	0	0	0	0	0	0
18	0	0	0	0	0	0	0	0	0	0	0	0	0	0	0	0	2	0	1	0	0	0	0	0	0	0	0	0	0	0	0	0	0	0	0	0	0	0	0	0	0
19	0	0	0	0	0	0	0	0	0	0	0	0	0	0	0	0	0	1	0	0	0	0	0	0	0	0	0	0	0	0	0	0	0	0	0	0	0	0	0	0	0
20	0	0	0	0	0	0	0	0	0	0	0	0	0	0	0	0	0	0	0	1	0	0	0	0	0	0	0	0	0	0	0	0	0	0	0	0	0	0	0	0	0
21	0	0	0	0	0	0	0	0	0	0	0	0	0	0	0	0	0	0	0	1	0	1	0	0	0	0	0	0	0	0	0	0	0	0	0	0	0	0	0	0	0
22	0	0	0	0	0	0	0	0	0	0	0	0	0	0	0	0	0	0	0	0	1	0	1	0	0	0	0	0	0	0	0	0	0	0	0	0	0	0	0	0	0
23	0	0	0	0	0	0	0	0	0	0	0	0	0	0	0	0	0	0	0	0	0	1	0	0	0	0	0	0	0	0	0	0	0	0	0	0	0	0	0	0	0
24	0	0	0	0	0	0	0	0	0	0	0	0	0	0	0	0	0	0	0	0	0	0	0	0	0	0	0	0	0	0	0	0	0	0	0	0	0	0	0	0	0
25	0	0	0	0	0	0	0	0	0	0	0	0	0	0	0	0	0	0	0	0	0	0	0	0	0	0	0	0	0	0	0	0	0	0	0	0	0	0	0	0	0
26	0	0	0	0	0	0	0	0	0	0	0	0	0	0	0	0	0	0	0	0	0	0	0	0	0	0	0	0	0	0	0	0	0	0	0	0	0	0	0	0	0
27	0	0	0	0	0	0	0	0	0	0	0	0	0	0	0	0	0	0	0	0	0	0	0	0	0	0	0	0	0	0	0	0	0	0	0	0	0	0	0	0	0
28	0	0	0	0	0	0	0	0	0	0	0	0	0	0	0	0	0	0	0	0	0	0	0	0	0	0	0	0	0	0	0	0	0	0	0	0	0	0	0	0	0
29	0	0	0	0	0	0	0	0	0	0	0	0	0	0	0	0	0	0	0	0	0	0	0	0	0	0	0	0	0	0	0	0	0	0	0	0	0	0	0	0	0
30	0	0	0	0	0	0	0	0	0	0	0	0	0	0	0	0	0	0	0	0	0	0	0	0	0	0	0	0	0	0	0	0	0	0	0	0	0	0	0	0	0
31	0	0	0	0	0	0	0	0	0	0	0	0	0	0	0	0	0	0	0	0	0	0	0	0	0	0	0	0	0	0	0	0	0	0	0	0	0	0	0	0	0
32	0	0	0	0	0	0	0	0	0	0	0	0	0	0	0	0	0	0	0	0	0	0	0	0	0	0	0	0	0	0	0	0	0	0	0	0	0	0	0	0	0
33	0	0	0	0	0	0	0	0	0	0	0	0	0	0	0	0	0	0	0	0	0	0	0	0	0	0	0	0	0	0	0	0	0	0	0	0	0	0	0	0	0
34	0	0	0	0	0	0	0	0	0	0	0	0	0	0	0	0	0	0	0	0	0	0	0	0	0	0	0	0	0	0	0	0	0	0	0	0	0	0	0	0	0
35	0	0	0	0	0	0	0	0	0	0	0	0	0	0	0	0	0	0	0	0	0	0	0	0	0	0	0	0	0	0	0	0	0	0	0	0	0	0	0	0	0
36	0	0	0	0	0	0	0	0	0	0	0	0	0	0	0	0	0	0	0	0	0	0	0	0	0	0	0	0	0	0	0	0	0	0	0	0	1	0	0	0	0
37	0	0	0	0	0	0	0	0	0	0	0	0	0	0	0	0	0	0	0	0	0	0	0	0	0	0	0	0	0	0	0	0	0	0	0	0	1	0	0	0	0
38	0	0	0	0	0	0	0	0	0	0	0	0	0	0	0	0	0	0	0	0	0	0	0	0	0	0	0	0	0	0	0	0	0	0	0	0	0	0	0	0	0
39	0	0	0	0	0	0	0	0	0	0	0	0	0	0	0	0	0	0	0	0	0	0	0	0	0	0	0	0	0	0	0	0	0	0	0	0	0	0	0	-2	0
40	0	0	0	0	0	0	0	0	0	0	0	0	0	0	0	0	0	0	0	0	0	0	0	0	0	0	0	0	0	0	0	0	0	0	0	0	0	0	-2	0	-4
41	0	0	0	0	0	0	0	0	0	0	0	0	0	0	0	0	0	0	0	0	0	0	0	0	0	0	0	0	0	0	0	0	0	0	0	0	0	0	0	-4	0

TABLE 4. Fractional Difference, in Parts Per Thousand, Between Curtis Matrix Elements Computed Using Line-by-Line and Interpolated Absorptivities for the 41-Level Pressure Grid Discussed in Section 6

	1	2	3	4	5	6	7	8	9	10	11	12	13	14	15	16	17	18	19	20	21	22	23	24	25	26	27	28	29	30	31	32	33	34	35	36	37	38	39	40	41
1	2	1	3	5	6	8	7	10	5	4	4	6	8	10	10	8	0	-15	4	29	11	-11	8	12	-4	14	14	16	18	21	21	22	23	24	25	25	26	26	28	25	0
2	1	0	0	0	0	1	1	2	0	0	0	1	2	4	3	2	-4	-14	-1	13	2	-12	0	2	-8	2	2	3	3	3	3	3	3	3	3	3	3	3	5	2	0
3	3	0	0	0	0	1	1	3	1	1	1	2	3	4	4	4	-1	-7	1	11	3	-6	2	3	-3	4	4	5	5	5	5	5	5	5	5	5	5	5	7	3	0
4	5	0	0	0	0	0	0	1	0	0	0	1	1	2	2	2	-1	-5	0	7	1	-4	0	1	-2	2	1	2	2	2	1	1	1	1	1	1	1	1	3	0	0
5	6	0	0	0	0	0	0	0	0	0	0	0	1	1	1	2	0	-3	0	5	1	-3	0	0	-1	1	1	2	1	1	0	0	0	0	0	0	0	0	2	-1	0
6	8	1	1	0	0	0	0	0	0	0	0	0	0	1	1	2	0	-2	0	3	1	-1	0	0	-1	0	0	1	1	0	0	0	0	0	0	0	0	0	2	-1	0
7	7	1	1	0	0	0	0	2	-10	0	0	1	1	1	1	2	0	0	1	3	1	0	1	1	0	1	1	2	2	1	0	0	0	0	0	0	0	0	2	-1	0
8	10	2	3	1	0	0	2	1	2	-2	0	0	0	0	0	1	0	-1	0	1	0	-1	0	-1	-1	0	0	0	0	-1	-1	-2	-2	-2	-1	-2	-2	-1	0	-3	0
9	5	0	1	0	0	0	-10	2	0	1	-6	0	0	0	0	1	0	-1	0	0	0	-1	-1	-1	-1	-1	-1	0	0	-1	-2	-2	-2	-3	-2	-3	-2	-2	0	-4	0
10	4	0	1	0	0	0	0	-2	1	0	2	-5	0	0	0	0	0	-1	0	0	0	-1	0	-1	-1	0	0	0	0	0	-1	-1	-1	-1	-1	-1	-1	-1	0	-3	0
11	4	0	1	0	0	0	0	0	-6	2	0	2	-7	0	0	0	0	-1	0	0	0	-1	0	0	-1	0	0	0	0	0	-1	-1	-1	-1	-1	-1	-1	-1	0	-3	0
12	6	1	2	1	0	0	1	0	0	-5	2	0	2	-10	0	1	0	0	0	0	0	0	0	0	0	0	0	0	0	0	0	-1	-1	-1	0	-1	0	0	1	-2	0
13	8	2	3	1	1	0	1	0	0	0	-7	2	0	4	-17	0	0	0	0	0	0	0	0	0	-1	0	0	0	0	-1	-1	-1	-1	-2	-1	-2	-1	-1	0	-3	0
14	10	4	4	2	1	1	1	0	0	0	0	-10	4	1	6	-25	0	0	0	0	0	0	0	0	-1	0	0	0	0	-1	-1	-1	-1	-2	-1	-2	-1	-1	0	-3	0
15	10	3	4	2	1	1	1	0	0	0	0	0	-17	6	2	9	-32	0	0	0	0	-1	-1	-1	-1	-1	-1	0	-1	-2	-3	-3	-3	-3	-2	-3	-3	-3	0	-5	0
16	8	2	4	2	2	2	2	1	1	0	0	1	0	-25	9	3	9	-26	1	0	0	0	0	0	0	0	0	2	1	1	0	0	0	0	1	0	0	0	3	-1	0
17	0	-4	-1	-1	0	0	0	0	0	0	0	0	0	0	-32	9	2	5	-14	0	0	0	0	0	0	0	0	0	0	0	-1	-1	-1	-2	-1	-2	-1	-1	0	-3	0
18	-15	-14	-7	-5	-3	-2	0	-1	-1	-1	-1	0	0	0	0	-26	5	1	3	-7	0	0	0	0	0	0	0	0	0	0	-1	-1	-1	-2	-1	-2	-1	-1	0	-3	0
19	4	-1	1	0	0	0	1	0	0	0	0	0	0	0	0	1	-14	3	0	3	-13	0	0	0	0	0	0	0	0	0	-1	-1	-1	-1	-1	-1	-1	-1	0	-3	0
20	29	13	11	7	5	3	3	1	0	0	0	0	0	0	0	0	0	-7	3	1	4	-16	0	0	0	0	0	0	0	0	-1	-1	-1	-1	-1	-1	-1	-1	0	-3	0
21	11	2	3	1	1	1	1	0	0	0	0	0	0	0	0	0	0	0	-13	4	1	4	-11	0	0	0	0	1	0	0	-1	-1	-1	-1	-1	-1	-1	-1	0	-2	0
22	-11	-12	-6	-4	-3	-1	0	-1	-1	-1	-1	0	0	0	-1	0	0	0	0	-16	4	1	2	-5	0	0	0	0	0	0	-1	-1	-1	-1	-1	-1	-1	-1	0	-2	0
23	8	0	2	0	0	0	1	0	-1	0	0	0	0	0	-1	0	0	0	0	0	-11	2	0	2	-9	0	0	1	0	0	-1	-1	-1	-1	-1	-1	-1	-1	0	-1	0
24	12	2	3	1	0	0	1	-1	-1	-1	0	0	0	0	-1	0	0	0	0	0	0	-5	2	0	0	1	0	0	0	0	-1	-1	-1	-1	-1	-1	-1	-1	0	-1	0
25	-4	-8	-3	-2	-1	-1	0	-1	-1	-1	-1	0	-1	-1	-1	0	0	0	0	0	0	0	-9	0	0	0	0	0	0	0	-1	-1	-1	-1	-1	-1	-1	-1	-1	-1	0
26	14	2	4	2	1	0	1	0	-1	0	0	0	0	0	-1	0	0	0	0	0	0	0	0	1	0	0	0	0	0	0	-1	-1	-1	-1	-1	0	-1	-1	-1	-1	0
27	14	2	4	1	1	0	1	0	-1	0	0	0	0	0	-1	0	0	0	0	0	0	0	0	0	0	0	0	0	-1	0	-1	-1	-1	-1	-1	0	-1	-1	-1	0	0
28	16	3	5	2	2	1	2	0	0	0	0	0	0	0	0	2	0	0	0	0	1	0	1	0	0	0	0	0	0	1	-1	0	0	0	0	0	0	0	-1	0	0
29	18	3	5	2	1	1	2	0	0	0	0	0	0	0	-1	1	0	0	0	0	0	0	0	0	0	0	-1	0	0	0	1	0	1	1	0	2	1	1	0	2	0
30	21	3	5	2	1	0	1	-1	-1	0	0	0	-1	-1	-2	1	0	0	0	0	0	0	0	0	0	0	0	1	0	0	0	-1	0	0	0	1	0	0	0	1	0
31	21	3	5	1	0	0	0	-1	-2	-1	-1	0	-1	-1	-3	0	-1	-1	-1	-1	-1	-1	-1	-1	-1	-1	-1	-1	1	0	0	0	-2	0	0	1	0	0	0	0	0
32	22	3	5	1	0	0	0	-2	-2	-1	-1	-1	-1	-1	-3	0	-1	-1	-1	-1	-1	-1	-1	-1	-1	-1	-1	0	0	-1	0	0	0	-5	-1	0	0	0	0	0	0
33	23	3	5	1	0	0	0	-2	-2	-1	-1	-1	-1	-1	-3	0	-1	-1	-1	-1	-1	-1	-1	-1	-1	-1	-1	0	1	0	-2	0	0	1	-13	1	0	0	0	0	0
34	24	3	5	1	0	0	0	-2	-3	-1	-1	-1	-2	-2	-3	0	-2	-2	-1	-1	-1	-1	-1	-1	-1	-1	-1	0	1	0	0	-5	1	0	1	-8	0	0	-1	0	0
35	25	3	5	1	0	0	0	-1	-2	-1	-1	0	-1	-1	-2	1	-1	-1	-1	-1	-1	-1	-1	-1	-1	-1	-1	0	0	0	0	-1	-13	1	0	1	-12	-15	0	0	0
36	25	3	5	1	0	0	0	-2	-3	-1	-1	-1	-2	-2	-3	0	-2	-2	-1	-1	-1	-1	-1	-1	-1	-1	0	0	0	2	1	1	0	1	-8	1	1	1	0	-18	-31	0
37	26	3	5	1	0	0	0	-2	-2	-1	-1	0	-1	-1	-3	0	-1	-1	-1	-1	-1	-1	-1	-1	-1	-1	-1	0	1	0	0	0	0	0	-12	1	0	0	19	-1	0
38	26	3	5	1	0	0	0	-1	-2	-1	-1	0	-1	-1	-3	0	-1	-1	-1	-1	-1	-1	-1	-1	-1	-1	-1	0	1	0	0	0	0	0	-15	0	0	0	-3	54	0
39	28	5	7	3	2	2	2	0	0	0	0	1	0	0	0	3	0	0	0	0	0	0	0	0	-1	-1	-1	-1	0	0	0	0	0	-1	0	-18	19	-3	-2	-8	0
40	25	2	3	0	-1	-1	-1	-3	-4	-3	-3	-2	-3	-3	-5	-1	-3	-3	-3	-3	-2	-2	-1	-1	-1	-1	0	0	2	1	0	0	0	0	0	-31	-1	54	-8	-4	0
41	0	0	0	0	0	0	0	0	0	0	0	0	0	0	0	0	0	0	0	0	0	0	0	0	0	0	0	0	0	0	0	0	0	0	0	0	0	0	0	0	0

In practice, p and p' are specified, either by the user or as the standard pressures of Table 1. Consequently we use (8*a*) and (8*b*) to obtain the pressures p_1 and p_2 for which $\tau(p_1, p_2; r_s)$ is approximately equal to $\tau(p, p'; r)$. We therefore obtain a first estimate for $\tau(p, p'; r)$ by employing the interpolation algorithm to obtain $\tau(p_1, p_2; r_s)$ and setting $\tau^{(\text{comp})}(p, p'; r) = \tau(p_1, p_2; r_s)$. The error due to this first approximation is remarkably small; as an illustration, transmissivities on the standard pressure grid have been computed for the CO_2 concentration of 495 ppmv using both the above method and the "exact" line-by-line technique. The fractional errors in absorptivity are always less than 2% and for most pressures are less than 1%.

A refinement of this procedure that allows use of the transmission functions at r_s', where $r_s' < r < r_s$, may be employed to improve accuracy, especially when $r \approx r_s'$. To do so, we compute the error $\tau(p, p'; r_s') - \tau^{(\text{exact})}(p, p'; r_s')$ obtained through use of the basic procedure. We now assume that this error varies linearly with $(r - r_s)$, and add this error to the previously computed value of $\tau(p, p'; r)$ to obtain our final answer. We may therefore write the approximation for nonstandard CO_2 concentrations as

$$\tau(p, p'; r) = \tau^{(\text{comp})}(p, p'; r) + \frac{(r_s - r)}{(r_s - r_s')} \cdot [\tau^{(\text{exact})}(p, p'; r_s') - \tau^{(\text{comp})}(p, p'; r_s')] \quad (9)$$

where $r_s' < r < r_s$.

This method may therefore be applied for any CO_2 concentration for which tabulated CO_2 transmissivities exist at concentrations greater and less than the given concentration. With this refinement the fractional errors in absorptivity for the 495-ppmv CO_2 mixing ratio case decrease to less than 1% for all pressures, with the typical error being less than 0.5%.

6. Validation of the Algorithm

We have computed by two approaches transmissivities for CO_2 concentrations of 330 ppmv on the 41-level pressure grid described in Table 2 of FS. This grid has pressures from 1000 to 10^{-2} mbar, fairly evenly spaced in geopotential height. The methods are (1) direct calculation and (2) the interpolation method of sections 3 and 4. Table 3 is the difference, in parts per thousand, in the absorptivity computed by each method. Point transmissivities have been used in this calculation. It is seen that the differences are never greater than 0.2%. A more stringent test is the comparison of Curtis matrix elements defined through the relation, $H_i = \sum B_j C_{ji}$, where H_i is the cooling rate due to the 15-μm band at pressure p_i and the sum is over all pressure levels. Table 4 is the difference in parts per thousand in the Curtis matrix elements computed on the above pressure grid. Again, the differences are small; errors are generally under 1%.

7. Summary of Available Tables

The authors will send a magnetic tape containing tables of line-by-line transmissivities and a program for computing interpolated transmissivities to any user upon request. The tables include 15-μm CO_2 transmissivities at concentrations of 330, 660, and 1320 ppmv. These are given with and without Planck weighting, enabling the user to select the transmissivities appropriate to his purpose. The interpolation program contains detailed documentation; at the user's option, either point or layer transmissivities may be computed.

The authors hope to update the line-by-line transmissivities periodically as better values for line strengths and widths become available. Also, the methods described in this paper will be applied to other bands, especially the CO_2 10-μm complex.

Appendix: Construction of the Analytic Function

A1. *Constraints on the Function*

The analytic function $A(p, p')$ defined in (4) and (5) has been constructed to represent, as closely as possible, the behavior of the actual CO_2 absorptivity $a(p, p')$ over a wide range of absorber amounts and pressures. (By actual CO_2 absorptivity we mean the 15-μm band CO_2 absorptivity computed by means of the line-by-line method discussed in section 2.) The choice of the functional form was motivated by the differing requirements for accuracy in various ranges of absorber amounts and pressures and by the need for simplicity, to permit rapid computation of transmissivities by this method.

As was indicated in section 3, the analytic function actually serves two rather different roles, depending on whether or not the pressure levels p and p' specified by the user are more closely spaced than the standard pressure levels. If they are, the analytic absorptivities $A(p, p')$ are used directly to compute $a(p, p')$; consequently the analytic function must be highly accurate. Yet it is precisely when $\Delta p \equiv |p - p'|$ is much smaller than the mean pressure $\bar{p}$ between p and p' that the needed accuracy is most difficult to attain. The problem in this case is that the transmissivity $\tau(p, p')$ varies nonlinearly with p and p' whenever $\Delta p/\bar{p}$ is small. In addition, the variation of $\tau(p, p')$ with Δp depends strongly on $\bar{p}$: as $\bar{p}$ increases from very small values, the CO_2 absorption lines pass from the Doppler regime to the nonoverlapped Lorentz regime and finally into the strongly overlapped limit. The need for accuracy is underscored by the fact that the largest contribution to the heating rate at pressure level p normally comes from the nearby pressure layers whose transmissivities have been evaluated through use of the analytic function. An additional complication in the case of small-absorber-path situations is that as $\Delta p \to 0$, the absorptivity as computed by the analytic function should tend to the weak line limit and be linear in absorber amount for all pressures $\bar{p}$. If the analytic function does not incorporate this weak line limit, fractional errors in absorptivity computed by this approach will rise uncontrollably as $\Delta p \to 0$.

If the pressure layers p and p' are more widely spaced than the standard pressure levels, $A(p, p')$ becomes an interpolator between appropriate values of $a(p_i, p_j)$ which have been precomputed using the LBL approach. In this situation the chief burden for accuracy is on the precomputed absorptivities, not the analytic function. Specifically, the analytic function is not required to possess the dependence on the logarithm of absorber amount given by experiment [*Howard et al.*, 1956]. It is important, however, that $A(p, p')$ vary smoothly for large $\Delta p/\bar{p}$ and that the analytically computed absorptivity increase monotonically as Δp increases.

In light of the above considerations, it is important to know the actual absorptivities for the small-path cases. To obtain these, we have computed LBL absorptivities for small paths over a wide range of $\bar{p}$. Details of the results are found in subsection A2. Using these results, we have constructed a function which (1) gives a close match to the LBL absorptivities for small paths, (2) approaches the correct weak line

limit as $\Delta p \to 0$, and (3) becomes a smooth function for interpolation in the case of large Δp. Details of this procedure are in subsection A3.

A2. *Line-by-Line Absorptivities in the Small-Path Case*

Line-by-line absorptivities have been computed for seven cases using the method described in section 2 and, in more detail, in the work of FS. In each case, one layer of the standard pressure grid was divided into 100 layers, each having the same mass and temperature. Transmissivities were computed between these narrowly spaced levels. The lowest pressure p_l, i.e., the lower of the two pressures on the standard pressure grid, was set at 0.01, 0.1, 1, 10, 100, ~315, and 1000 mbar for the successive experiments These calculations have the effect of extending to ~0.0015 scale height the transmissivity calculations of section 2 at the specified pressures.

The results of these runs provide seven curves relating absorptivity to absorber amount. In Figure 1 we plot the logarithm of absorptance between the lowest pressure level and the other pressure levels (log $a(p', p_l)$) versus the logarithm of the corresponding absorber mass, normalized by the absorber mass between successive levels of the standard pressure grid (log $[m(p', p_l)/m(p_{l+1}, p_l)]$). For convenience, Figure 2 displays the relation between absorptivity ($a(p', p_l)$) versus the same normalized absorber amount.

Inspection of Figures 1 and 2 reveals a number of distinct regimes. When p_l is ~315 or 1000 mbar, the absorption is nearly proportional to the logarithm of absorber mass, particularly for the largest values of Δp. This result is consistent with experimental results [*Howard et al.*, 1956; *Gryvnak et al.*, 1976] on larger paths. For smaller pressures it appears that log $a(p', p_l)$ is, to a good approximation, proportional to log (Δp), and thus $a(p', p_l) \propto (\Delta p)^k$. The exponent k appears to be very nearly 0.55 for the cases where p_l is between 1 and 100 mbar. If p_l is 0.01 mbar, to a good approximation, $a(p', p_l) \propto (\Delta p)^{0.95}$ for very small Δp, and $a \propto (\Delta p)^{0.47}$ for the larger values of Δp.

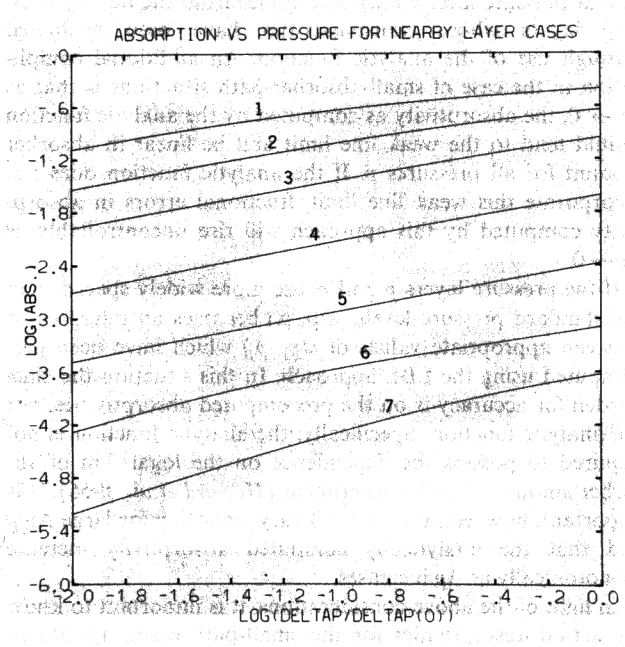

Fig. 1. Line-by-line absorptivities as a function of absorber masses for the seven small-path cases described in the appendix. The ordinate is $\log_{10} a(p_l, p_l + \Delta p)$, with $p_l = 0.01$, 0.1, 1, 10, 100, 315, and 1000 mbar. The abscissa is $\log_{10} (\Delta p/\Delta p_0)$ where $\Delta p_0 = p_{l+1} - p_l$ for each case; the values of all pressures are given in Table 1. The respective cases are designated as 1, 2, 3, 4, 5, 6, and 7.

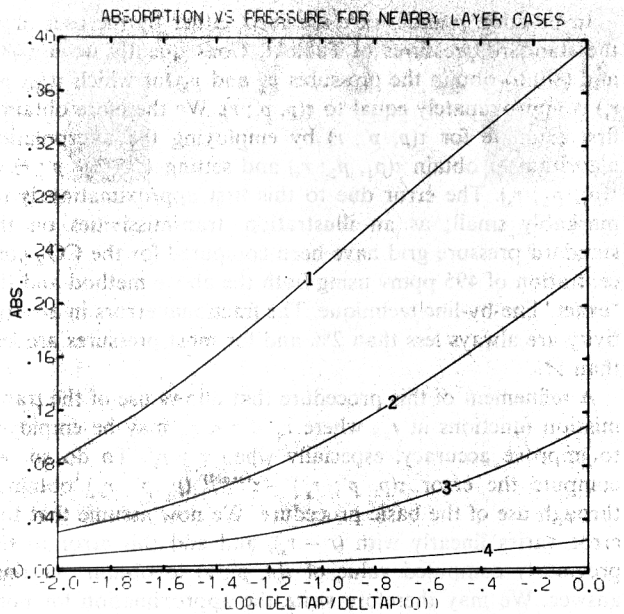

Fig. 2. The same as Figure 1, but with the ordinate being $a(p_l, p_l + \Delta p)$.

It is worthwhile to examine whether or not these complex relationships could be anticipated from simple theoretical considerations. First, we note that the very low mass and pressure absorption curves, for which the absorption is almost proportional to Δp, represent the onset of the weak line limit. The deviations from linearity are presumably caused by the influence of a few CO_2 lines not totally in this limit. On the other hand, the absorption curves at 315 and 1000 mbar represent the strongly overlapped Lorentz regime. In this situation it may be shown [see *Tiwari*, 1978] that absorptivity does tend to be proportional to the logarithm of absorber amount.

The remaining cases lie in the transitional region between weak line and logarithmic behavior. For mean pressures of $\lesssim$30 mbar, individual CO_2 lines may be taken to be nonoverlapped Lorentzian lines. In this situation we are in the large-path limit, so that we expect $a \propto (\bar{p}\Delta p)^{0.5}$. For smaller pressures, the individual lines enter the Doppler regime. In this case, as is shown by *Fels* [1984, p. 1759], the relation between absorptivity and absorber amount depends crucially on the actual distribution of CO_2 line strengths; as is discussed in that paper, a realistic choice of the distribution, for those strengths contributing most to the absorption at the particular mass, leads to a dependence of the absorption on approximately the square root of absorber mass, or $a \propto (\Delta p)^{0.5}$. These estimates are close to the measured dependence. In a future note we intend to discuss in greater detail the significance of the deviations from these theoretical expectations.

A3. *Determination of the Analytic Function*

The above results indicate that our analytic function $A(p, p')$ for absorptivity should be constrained to approach the following limits:

1. In the Doppler regime, $A(p, p') \propto \Delta p$ for very small Δp, and $A(p, p') \propto (\Delta p)^j$ for large Δp, with j being slightly less than 0.5,
2. In the nonoverlapped Lorentz regime, $A(p, p') \propto (\bar{p}\Delta p)^k$, with k somewhat greater than 0.5,
3. In the overlapped Lorentz regime, $A(p, p') \propto [\log (\bar{p}\Delta p)]^l$, with l near 1.0.

We may simplify the above relations by defining a single path function $U(p, p')$ whose value is proportional to Δp in the Doppler limit and to $\bar{p}\Delta p$ in the Lorentz limit. This path function, roughly speaking, corresponds to the pressure-weighted absorber amount between p and p'.

As was mentioned earlier, the analytic function must not only be accurate for small $\Delta p/\bar{p}$, conforming to the constraints of the preceding discussion, but also serve as an interpolation for large $\Delta p/\bar{p}$. A functional form encompassing both purposes is given by

$$A(p, p') = \{C(p) \log [1 + X(p)U(p, p')^{\delta}]\}^{(\gamma/\delta)} \tag{A1}$$

In (A1), C and X are empirical coefficients which are not functions of the path and are taken to be functions of the pressure at p. Their function is to permit use of the analytic function as an interpolator.

Equation (A1) has the following desirable limits: when $X(p)U(p, p') \gg 1$,

$$A(p, p') \propto [\log U(p, p')]^{(\gamma/\delta)} \tag{A2a}$$

when $X(p)U(p, p') \ll 1$,

$$A(p, p') \propto U(p, p')^{\gamma} \tag{A2b}$$

The experimental constraints given at the beginning of this section may then be satisfied if (1) $U(p, p') \propto (\bar{p}\Delta p)$ in the Lorentz regime, for both large and small Δp; (2) $U(p, p') \propto \Delta p$ in the Doppler regime, with relatively large Δp; and (3) $U(p, p') \propto (\Delta p)^{1/\gamma}$ in the Doppler regime, with small Δp.

In this third case, moreover, we may determine the constant of proportionality by requiring that the absorptivity for very small Δp be equal to that obtained in the theoretical weak line limit:

$$A(p, p') = m\frac{S}{\Delta\nu} = \frac{rd\Delta p}{g}\frac{S}{\Delta\nu} \tag{A3}$$

(In the above equation, r is the CO_2 mixing ratio, d is the diffusivity factor, g is the gravitational constant, and S is the summed CO_2 line intensities over the frequency range $\Delta\nu$.) Equating (A3) and (A1), under the constraint of (A2b), we obtain the path function in the weak line limit

$$U(p, p') = \eta^{-1}(\Delta p)^{1/\gamma} \tag{A4a}$$

with

$$\eta = \left(\frac{rdS}{g\Delta\nu}\right)^{-1/\gamma} [C(p)X(p)]^{(1/\delta)} \tag{A4b}$$

The remaining task is the determination of the actual form of $U(p, p')$, subject to the above limits. After some experimentation, the following expression has been obtained:

$$U(p, p') = \frac{(\Delta p)^{1/\gamma}(p + p' + \text{core})}{\eta(p + p' + \text{core}) + \Delta p^{(1/\gamma - 1)}} \tag{A5}$$

In (A5), "core" is a parameter determining the limit of the Doppler and Lorentz regimes; i.e., the Doppler regime is that for which core $>(p + p')$. The above relation reduces to the weak line expression of (A4a) if $\Delta p^{[(1/\gamma)-1]} \ll \eta(p + p' + \text{core})$. On the other hand, if $\eta(p + p' + \text{core}) \ll \Delta p^{[(1/\gamma)-1]}$, then $U(p, p') \approx \Delta p(p + p' + \text{core})$, and therefore $U(p, p') \approx \Delta p(p + p')$ in the Lorentz regime, and $U(p, p') \approx \Delta p(\text{core})$ in the Doppler regime. The three constraints on $U(p, p')$ are thus satisfied by the definition of $U(p, p')$ in (A5).

The remaining task is the specification of the experimental parameters core, γ, and δ and the evaluation of C, X, and η. After considerable experimentation, the following values of core, γ, and δ have been adopted:

$$\text{core} = 5 \tag{A6a}$$

$$\delta = 0.90 \tag{A6b}$$

$$\gamma(p) = 0.505 + (2 \times 10^{-5})p + 0.035\left(\frac{p^2 - 0.25}{p^2 + 0.25}\right) \tag{A6c}$$

with p expressed in millibars. According to (A6c), $\gamma(p)$ varies between 0.56 at $p = 1000$ mbar and 0.47 at $p = 10^{-3}$ mbar. The change is approximately linear in p but is more rapid near 1 mbar, where the transition from Lorentz to Doppler profile takes place.

The values of δ and $\gamma(p)$ chosen above lead to a long-path limit of $A(p, p') \propto \log (\bar{p}\Delta p)^l$ with l of $\sim$0.6 rather than unity. We have chosen these values because they result in the most accurate computations of transmissivities in the case of large pressures and small absorber amounts. When absorber amounts become comparable to $m(p_l, p_{l+1})$, the accuracy using the present values of δ and γ is almost identical to that obtained with l of $\sim$1.0. There are two reasons for this. First, as $m(p', p_l) \rightarrow m(p_{l+1}, p_l)$, the approximation function is constrained to become exact, and therefore any choice of γ and δ will not introduce error. Second, when $m(p', p_l)$ is much less than $m(p_{l+1}, p_l)$, an absorption formula of the form $a \propto \log (\bar{p}\Delta p)^l$ is, in practice, rather insensitive to the value of l, provided that l lies between 0.5 and 1.0.

An iterative procedure is used to determine C, X, and η on the standard pressure grid. A first guess is taken for $\eta(p_i)$, and $C(p_i)$ and $X(p_i)$ are computed by using (A1) with the following conditions:

$$A(p_i, p_{i-1}) = a(p_i, p_{i-1})$$

$$A(p_i, p_{i-2}) = a(p_i, p_{i-2})$$

A new value for $\eta(p_i)$ is obtained using (A4b), and the procedure is repeated until $C(p_i)$, $X(p_i)$, and $\eta(p_i)$ converge.

The use of (A4b) to compute η involves a number of con-

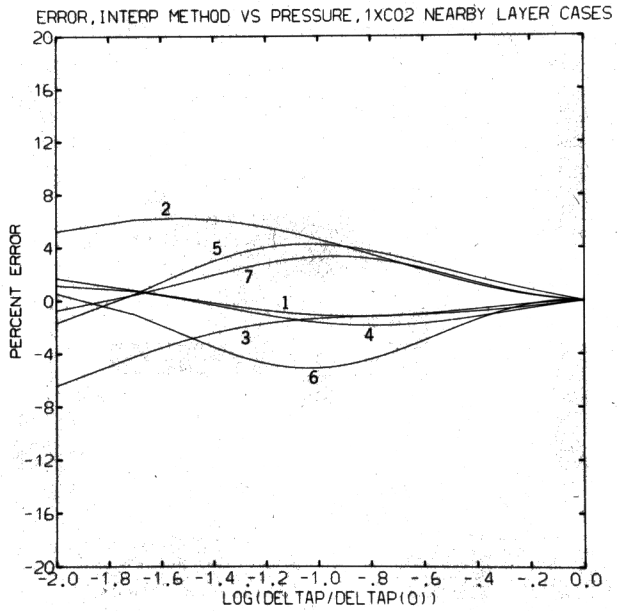

Fig. 3. Fractional error (a(interp) − a(LBL)/a(LBL)) using the new interpolation algorithm for the seven small-path cases described in the appendix. A CO_2 mixing ratio of 330 ppmv is used. The cases are numbered as in Figure 1.

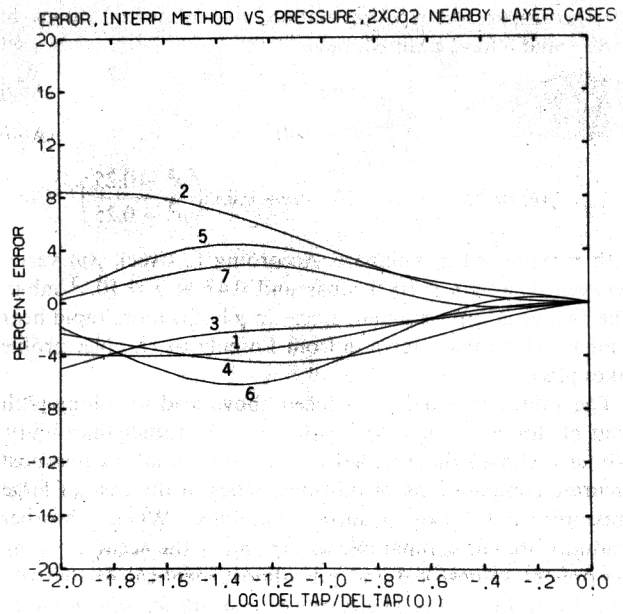

Fig. 4. Same as Figure 3, with a CO_2 mixing ratio of 660 ppmv employed.

siderations. First, η is a function of the CO_2 mixing ratio. In addition, the summed CO_2 line strength is assumed constant at all temperatures, a valid assumption for the 15-μm band in the 500–850 cm^{-1} frequency band. The diffusivity factor d, which may vary between 1.66 and 2.00, has been fixed at 2.00 to provide good agreement between line-by-line and computed absorptivities in the weak line limit.

Equation (A1) has been employed to compute absorptivities for each of the seven small-path cases described earlier in section A2. Figure 3 displays the fractional error obtained in each case with the CO_2 mixing ratio of 330 ppmv; Figure 4 gives corresponding results for a 660-ppmv CO_2 mixing ratio. In every case the fractional errors are under 8%. These errors are sufficiently small to justify use of this formulation for small paths over a wide range of mean pressures.

Acknowledgments. S. Manabe and D. Crisp provided helpful comments. J. Kennedy repeatedly and skillfully typed the manuscript. The comments of two anonymous reviewers have been very useful.

REFERENCES

Fels, S. B., The radiative damping of short vertical scale waves in the mesosphere, *J. Atmos. Sci.*, *41*, 1755–1764, 1984.

Fels, S. B., and M. D. Schwarzkopf, An efficient, accurate algorithm for calculating CO_2 15-μm band cooling rates, *J. Geophys. Res.*, *86*(C2), 1205–1232, 1981.

Gryvnak, D. A., and D. E. Burch, Infrared absorption by CO_2 and H_2O, *Rep. AFGL-TR-78-0154*, Air Force Geophys. Lab., Hanscom Air Force Base, Bedford, Mass., 1978.

Gryvnak, D. A., D. E. Burch, P. L. Alt, and D. K. Zgonc, Infrared absorption by CH_4, H_2O and CO_2, *Rep. AFGL-TR-76-0246*, Air Force Geophys. Lab., Hanscom Air Force Base, Bedford, Mass., 1976.

Howard, J. N., D. E. Burch, and D. Williams, Infrared transmission of synthetic atmospheres, 2, Absorption by carbon dioxide, *J. Opt. Soc. Am.*, *46*, 237–241, 1956.

Rothman, L. S., AFGL atmospheric absorption line parameters compilation: 1980 version, *Appl. Opt. 20*, 791–795, 1981.

Tiwari, S. N., Models for infrared atmospheric radiation, *Adv. Geophys.*, *20*, 1–85, 1978.

World Climate Programme, The intercomparison of radiation codes in climate models (ICRCCM) - Longwave clear-sky calculations, *Rep. WCP-93*, Prepared by F. M. Luther, World Meteorological Organization, Geneva, Italy, 1984.

S. B. Fels and M. D. Schwarzkopf, Geophysical Fluid Dynamics Laboratory/NOAA, Princeton University, P. O. Box 308, Princeton, NJ 08542.

(Received January 17, 1985;
revised June 27, 1985;
accepted July 1, 1985.)